DESIGN CONSIDERATIONS FOR SHAPE MEMORY POLYMER COMPOSITES WITH MAGNETO-SENSITIVE PARTICLES

P. H. Kao, K.K. Westbrook, Francisco Castro, H.J. Qi*
Department of Mechanical Engineering, University of Colorado, Boulder, CO, USA
* Corresponding author(qih@colorado.edu)

Keywords: *Shape Memory Behaviors; Shape Memory Polymers; Active Materials*

1. Introduction

Shape memory polymers (SMPs) are a group of adaptive polymers that can recover the permanent shape from a temporary shape by external stimuli on demand. Among a variety of external stimuli for polymer actuation, temperature is the commonly used. However, due to slow heating rates, recovery of this type of SMP is usually slow. Recently, efforts have been made to improve the recovery rate of SMPs by using novel heating methods. For example, the SM effect is realized through converting electrical energy to heat through magnetic field induced inductive heating of magnetic particles dispersed in an SMP. This approach offers the advantages of fast and remote heating. In this paper, we investigate the considerations in designing mageno-sensitive particle reinforced SMPs using finite element simulations enhanced by a newly developed thermomechanical finite deformation constitutive model. In particular, we study the influence of particle size, particle volume fraction, heating temperature to the recovery rate of SMP.

2. Model Description

2.1 Shape Memory Polymers

Shape memory polymers (SMPs) are a class of polymers capable of demonstrating large recoverable shape changes due to an environmental stimulus, such as temperature [1, 2], light [3, 4], magnetic field [5, 6]. The latter can be thought of as indirect thermally triggered behavior. The first and most widely studied class of SMPs is thermally triggered. A typical thermomechanical history during an SM cycle includes two steps (Fig. 1): a programming (or shape fixing) step and a recovery (or deploying) step. In the programming step, the polymer first is deformed at a temperature above its glass transition temperature (T_g) into the desired deformed state. This is followed by cooling the polymer down to a temperature below T_g while maintaining the initial deformation constraint. The recovery step, the polymer is heated to a temperature above T_g. Depending on the application where the recovery strain or stress is important, heating can be either under free or constrained conditions respectively.

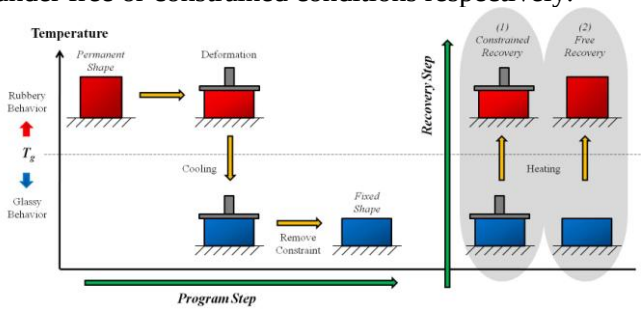

Fig 1. A schematic depicting the thermomechanical history for a shape memory cycle showing the two steps of programming (shape fixing) and recovery (deploying) under both a constrained and free recovery scenario.

2.2 Constitutive Model for SMP

Recently, a multi-branch model is developed by the authors to capture the SM effect by considering the complex thermomechanical properties of amorphous SMPs as the temperature crosses T_g. Fig. 2 shows the 1D rheological representation of the model.

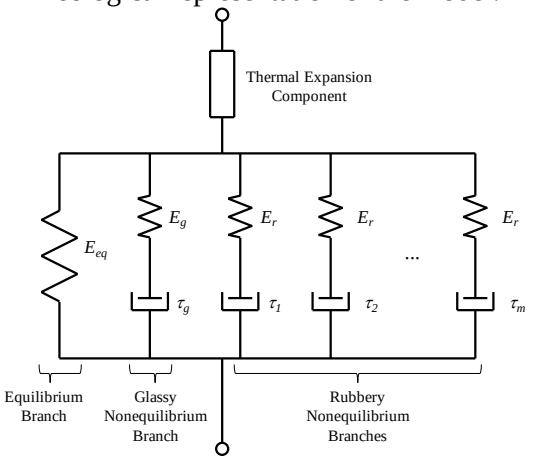

Fig. 2. 1D rheological representation of the constitutive model for SMP.

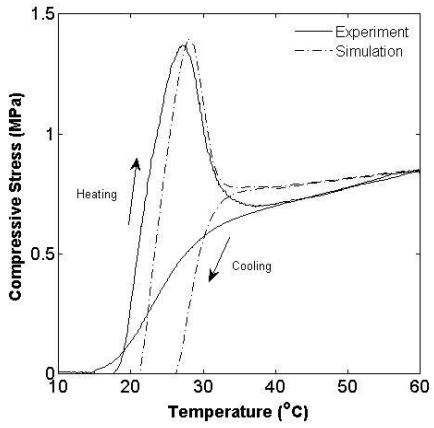

(A)

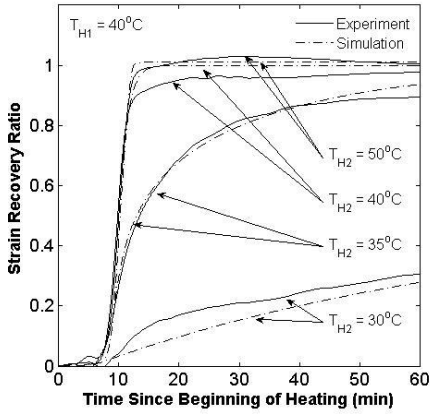

(B)

Fig. 3. Comparison between numerical simulation and experimental results (A) for the stress response during a constrained recovery (b) the strain recovery during a free recovery at different recovery temperatures for a programming temperature of T_{H1} = 40°C.

In Fig. 2, the mechanical elements consist of an equilibrium branch and several nonequilibrium branches. Each nonequilibrium branch is a nonlinear Maxwell element. In the set of nonequilibrium branches, only one is used to represent the relaxation behavior of the glassy mode, which describes the structural or segmental relaxation of polymers and defines the monomer friction coefficient which in term enslaves all the longer time scale chain relaxation processes. The remaining nonequilibrium branches are used to represent the relaxation processes in the rubbery state (or melt state), which can be represented by a series of Rouse modes. The detailed description of the model can be found in Westbrook et al. [7]. The comparison of the free recovery behavior between experiments and model simulations is shown in Fig. 3 for the case of constrained recovery (Fig. 3A) and free recovery (Fig. 3B). It can be seen that the model captures very well the experimentally observed shape memory behavior in SMP.

2.3 Finite element model of magneto-sensitive SMP composites

Recently, efforts have been made to improve the recovery rate of SMPs by using novel heating methods. For example, the SM effect is realized through the inductive heating of magnetic particles dispersed in an SMP [8, 9]. This approach offers two potential advantages for shape recovery. First, heating the material can be achieved remotely by alternating a magnetic field. Second, the heating rate of the SMP structure can be significantly increased. Besides these advantages, the inclusions of particles in SMPs [5, 10] allows for medical imaging techniques, such as fluoroscopy or computed tomography scans, to detect the implanted device without additional surgeries for proper device placement and function.

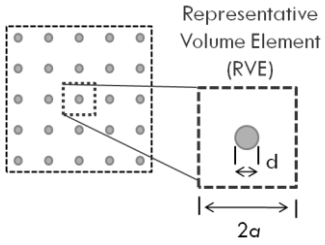

(A)

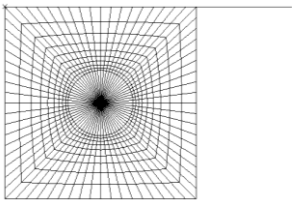

(B)

Fig. 4. Representative volume element (RVE) for a magnetosensitive SMP composite. (A) 2D cross-section schematic showing the RVE for the periodic problem. (B) Finite element model mesh for the RVE for a filler volume fraction of 10% and a filler diameter of 10 μm.

Here, we consider the effect of particle size and volume fraction on the free recovery behavior of a magnetosensitive SMP composite. In particular, we assume that the particles can be heated to the

targeted temperature immediately and be maintained at that temperature. The heat is then transferred into the SMP matrix to trigger the recovery. The effect of particle size on the shape recovery time is investigated. Assuming uniform particle dispersion, a representative volume element (RVE) is modeled in a 2D setting as shown in Fig. 4A. Although the 2D model may represent a long fiber filler, the general insight from this model can be extended to particles. The filler volume fraction can be related to the RVE geometry by

$$\phi_{2D} = \frac{V_{filler}}{V_{matrix}} = \frac{\pi d^2}{4(2a)^2 - \pi d^2}$$

where d is the diameter of the filler and $2a$ is the RVE edge length as shown in the schematic in Fig. 2A. In the parametric studies for a given filler volume fraction, the filler diameter is varied over many decades and the corresponding RVE edge lengths are calculated.

Using the geometry of the RVE, finite element models that couple heat transfer with finite deformation solid mechanics were created. For the SMP matrix, 4-node bilinear displacement and temperature, hybrid with constant pressure elements (CPE4HT) in Abaqus element library were used; for the filler, 3-node linear displacement and temperature elements (CPE3T) were used. A representative finite element mesh is shown in Fig. 4B for a 10% volume fraction and a filler diameter of 10 μm. Periodic boundary conditions (PBCs) [11, 12] were applied by using equation constraints for the edge nodes. Because of the PBCs, the initial compressive displacement is applied on the RVE's top left node. Additionally, to account for the thermal contraction during cooling, an analytic rigid surface was included so the top left node vertical displacement boundary condition could be removed after the initial compression. Here the programming, fixing were 40 °C, 20 °C, respectively for all the cases. The recovery temperature were 40°C and 50°C, respectively. Following Westbrook et al. [13] it is assumed the SMP has a heat capacity, density and conductivity of 640 J/(kg °C), 1050 kg/m^3 and 0.15 W/(m °C), respectively. During the cooling step, the nodal temperature (SMP and filler) are prescribed; whereas, to account for instantaneously heating, the temperature of the particle nodes are ramped to the recovery temperature in 0.1 milliseconds.

3. Results

Fig. 5 shows the effects of changing the diameter for three volume fractions, 0.1%, 1% and 10%. Here, the time for full recovery is taken to be when the recovery ratio reaches 95%. As seen in Fig. 3, for each volume fraction, there exists a critical diameter, below which the time for recovery is independent of the filler size. The critical diameters for the 0.1 %, 1 % and 10% volume fractions are approximately 2 μm, 10 μm and 95 μm for recoveries at 50°C, and 20 μm, 80 μm and 900 μm for recoveries at 40°C, respectively. The existence of a critical filler size represents a transition of recovery from one dominated by heat transfer to one dominated by material intrinsic recovery. At the same filler volume fraction, decreasing filler diameter reduces the RVE size and thus effectively reduces the length of the pathway for heat transfer. Below a critical filler size, the size of the RVE becomes unimportant as heating can occur almost instantaneously. Therefore from heating efficiency and material recovery points of view, it is unnecessary to further reduce the filler size.

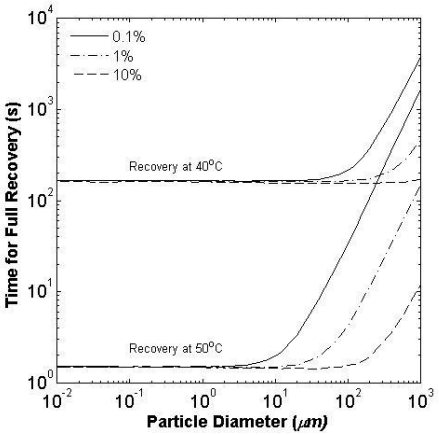

Fig. 5. Free recovery time as a function of the size magnet-sensitive particle size.

4. Conclusion

This paper considers the improved recovery of SMP by using magneto-sensitive particles. Through simulation, we found there exists a critical particle size, below which reducing particle size will not improve recovery rate.

Acknowledgement

We gratefully acknowledge the support of an NSF career award (CMMI-0645219), an AFOSR grant

(FA9550-09-1-0195; Dr. Les Lee, program manager).

References

1. Gall, K., et al., *Thermomechanics of the shape memory effect in polymers for biomedical applications.* Journal of Biomedical Materials Research Part A, 2005. **73A**(3): p. 339-348.
2. Mather, P.T., X. Luo, and I.A. Rousseau, *Shape Memory Polymer Research.* Annual Review of Materials Research, 2009. **39**: p. 445-471.
3. Lendlein, A., et al., *Light-induced shape-memory polymers.* Nature, 2005. **434**(7035): p. 879-882.
4. Scott, T.F., et al., *Photoinduced plasticity in cross-linked polymers.* Science, 2005. **308**(5728): p. 1615-1617.
5. Buckley, P.R., et al., *Inductively heated shape memory polymer for the magnetic actuation of medical devices.* Ieee Transactions on Biomedical Engineering, 2006. **53**(10): p. 2075-2083.
6. Schmidt, A.M., *Electromagnetic activation of shape memory polymer networks containing magnetic nanoparticles.* Macromolecular Rapid Communications, 2006. **27**(14): p. 1168-1172.
7. Westbrook, K.K., et al., *A 3D Finite Deformation Constitutive Model for Amorphous Shape Memory Polymers: A Multi-Branch* 2011. **submitted**.
8. Madbouly, S. and A. Lendlein, *Shape-Memory Polymer Composites*, in *Shape-Memory Polymers*. p. 41-95.
9. Weigel, T., R. Mohr, and A. Lendlein, *Investigation of parameters to achieve temperatures required to initiate the shape-memory effect of magnetic nanocomposites by inductive heating.* Smart Materials and Structures, 2009. **18**(2): p. 025011.
10. Yakacki, C.M., et al., *Shape-memory polymer networks with fe3O4 nanoparticles for remote activation.* Journal of Applied Polymer Science, 2009. **112**(5): p. 3166-3176.
11. van der Sluis, O., et al., *Overall behaviour of heterogeneous elastoviscoplastic materials: effect of microstructural modelling.* Mechanics of Materials, 2000. **32**(8): p. 449-462.
12. Bertoldi, K., et al., *Mechanics of deformation-triggered pattern transformations and superelastic behavior in periodic elastomeric structures.* Journal of the Mechanics and Physics of Solids, 2008. **56**(8): p. 2642-2668.
13. Westbrook, K.K., et al., *Improved testing system for thermomechanical experiments on polymers using uniaxial compression equipment.* Polymer Testing, 2010. **29**(4): p. 503-512.